Available free online at www.medjchem.com

Mediterranean Journal of Chemistry

Mediterranean Journal of Chemistry **2022**, 12(2), 149-163

Elimination of Terbinafine Hydrochloride Antifungal Drug Traces from Water, Pharmaceutical Formulations and Blood Plasma using Low-Cost Bio and Synthetic Sorbents

Samah Ali [1,2], Bushra Alharbi [1] and Amr Mohamed [1, 3, *]

[1] Chemistry Department, College of Science, Taibah University, Al-Madinah Al-Munawarah, Saudi Arabia
[2] The National Organization for Drug Control and Research, Al-Agouzah, Giza, Egypt
[3] The Higher Institute of Optics Technology (HIOT), Heliopolis 17361, Cairo, Egypt

Abstract: Chitosan (CS) biosorbent and polyurethane foam (PUF) synthetic sorbent have been utilized to eliminate terbinafine hydrochloride (TRB HCl) antifungal drug in its pure and pharmaceutical forms from both contaminated aqueous and biological media using a batch process. The experimental conditions for efficient removal of TRB HCl for both CS and PUF were optimized depending on various experimental parameters such as the pH of the solution, contact periods, initial TRB HCl concentration, and sorbents dosage in the solution.

SEM, FT-IR, and XRD characterizations were carried out to study the adsorption of a drug by both sorbents. The optimum conditions for removing TRB HCl by CS and PUF were achieved at a pH of 8.5 and a contact time of 60 min at 250 rpm, using 0.4 g for both sorbents. The measured spectrophotometric absorbance at λ_{max} of TRB HCl was 242 nm. In addition, the zero-point charge (pHpzc) was determined for the studied sorbents. The pHpzc of the surface of sorbents has shown that electrostatic attraction is one of the mechanisms in TRB HCl sorption. The adsorption process was modeled using the pseudo-first-order, pseudo-second-order, Elovich, and intraparticle diffusion kinetic models. The results indicated that the adsorption of TRB HCl on CS and PUF does follow a pseudo-first-order type of reaction kinetics. The adsorption process was modeled using Langmuir and Freundlich isotherms. The adsorption data found that the Freundlich isotherm model was more suitable for the PUF sorbent, while the Langmuir isotherm model better fit the CS biosorbent.

Evaluation of the experimental data using the Langmuir equation revealed that the maximum adsorption capacities of PUF and CS were 2.807 and 1.2297 mg. g^{-1}, respectively. The solution was also used to estimate TRB HCl in its pharmaceutical form, and the assessed recoveries were 97.25 and 98.437% for CS and PUF, respectively. The proposed procedure was also validated for other complex mediums by removing TRB HCl from spiked human blood plasma. *In-silico* aquatic toxicity forecast of TRB HCl was also carried out.

Keywords: chitosan biosorbent (CS); polyurethane foam synthetic sorbent (PUF); terbinafine hydrochloride antifungal (TRB HCl); pharmaceuticals; blood plasma.

1. Introduction

Significant amounts of harmful pollutants continuously enter the food chain, especially via contaminated water, and bioaccumulate in the living organisms [1,2]. For example, the European Executive Agency for Health and Consumers (EAHC) has previously reported that the annual worldwide consumption of drugs is estimated to be about 100,000 tons/year [3]. These drugs are finally being discovered in surface and sewage water, soils, sludge, and air, affecting the whole ecosystem and, consequently, human health, mainly upon long-term exposure to low pharmaceuticals [4,5].

Terbinafine hydrochloride (TRB HCl) [$C_{21}H_{26}ClN$] is a synthetic allylamine antifungal agent [6]. Heavy doses of TRB HCl can cause several effects, such as allergic reactions, breathing difficulties, the closing of the throat and swelling of the hips, tongue, face, and liver, rashes, changes in vision, and blood problems [7]. TRB HCl also has long-lasting harmful effects on aquatic life under some ecological conditions [8]. As an example, TRB HCl was detected in the water of India wells at concentrations higher than 1 $\mu g.L^{-1}$, and it was also isolated there from lakes and rivers [9]. Various methods for determining terbinafine in drugs, pharmaceuticals, body fluids, and other biological matrices have been previously described [7]. Those methods include UV-spectrophotometry [10],

**Corresponding author: Amr Mohamed*
Email address: addeck@taibahu.edu.sa
DOI: http://dx.doi.org/10.13171/mjc02209271644amr

Received August 3, 2022
Accepted August 24, 2022
Published September 27, 2022

HPTLC [11,12], voltammetric [13] and non-aqueous methods [14], visible spectrophotometry [15], spectrofluorimetry [16], electrochemical methods [17], capillary electrophoresis [18] and LC/MS [19].

Amongst the several contaminants-removal techniques, sorption is one of the most common processes for transferring water contaminants into a solid phase because of its efficiency, comparatively lower costs, high removal capacity, and ease of application [20-23]. Biosorbents can be any plant, animal, microbial biomass or their derivatives, agriculture wastes, and byproducts of industries [24,25]. Biosorbents have many advantages over traditional adsorbents, such as availability, low costs, attractive adsorption efficiency, simple operation, good reuse, and the absence of the formation of secondary pollutants [26].

Chitosan (CS) is a natural polymer biosorbent composed of randomly distributed β-(1-4)-linked D-glucosamine (deacetylated unit) and N-acetyl-D-glucosamine (acetylated unit) [27]. It can be commercially produced from chitin, the main component of crustacean shells, mostly from shrimp processing wastes [28-30]. It is an attractive water treatment biosorbent with hydrophilic properties and nontoxicity, yet it's environmental-friendly with high adsorption capabilities [31,32]. Chitosan can effectively function as a nontoxic polycationic coagulating agent in wastewater treatment [33,34].

Polyurethane foam (PUF) is a synthetic sorbent for solid-phase extraction applications [35]. It can remove polar and non-polar pollutants from water because of its hydrophobic and oleophilic characteristics [36,37].

PUF has multiple advantages as a sorbent, including high surface area, low cost [38], chemical inertness, mechanical strength [39], high porosity, and open-cell [40], in addition to its low density [41]. Moreover, PUF has a significant chemical resistance, thermal stability, and the ability to retain various substances within its framework [42].

In this study, chitosan biosorbent (CS) and polyurethane foam synthetic sorbent (PUF) has been employed for the elimination of terbinafine hydrochloride (TRB HCl) from different aqueous media. The sorption-influencing parameters, such as pH, contact time, initial TRB HCl concentration, amount of sorbents, and isotherm modeling studies, were investigated. The proposed method was also validated for the application on blood plasma as an example of complex natural matrices. This study also carried out the in-silico computational aquatic toxicity forecast of TRB HCl.

2. Materials and Methods

2.1. Instrumentation

All spectrophotometric measurements of TRB HCl were performed using a UV-Visible spectrophotometer with a quartz cell. The pH measurements were carried out using a pH meter from HANNA Instruments. The morphology of both sorbents was studied using scanning electron microscopy (SEM) before and after the adsorption of the TRB HCl drug. Fourier transform-infrared (FT-IR) spectroscopic characterization and X-ray diffraction (XRD) analysis were carried out for free and drug-loaded sorbents.

2.2. Reagents and materials

All chemical reagents were used without prior purification. Hydrochloric acid 37% was from Panreac Applichem Co. Sodium phosphate monobasic, sodium phosphate dibasic, and sodium acetate were purchased from Fisher Biotech Co. All solutions were prepared with double-distilled water. Terbinafine hydrochloride (TRB HCl) was obtained from the National Organization for Drug Control and Research (NODCAR), Cairo, Egypt. The Open-cell polyether-type PUF (d = 31.6 $kg.m^{-3}$, moisture content = 2.7%), was supplied by the Egyptian Company for Foam Production, Cairo, Egypt. Chitosan was purchased from Al-Alamia Company for Chemicals, Cairo, Egypt (d = 0.15 $g.mL^{-1}$, moisture content = 8.2%). All chemicals were obtained from Aldrich Chemical Company.

The pH of the samples was adjusted using acetate and phosphate buffer. Stock solutions of TRB HCl (100 ppm) were prepared by dissolving 0.25 mg diluting to 250 mL by water. All laboratory glassware was soaked overnight in chromic acid solution. Commercial pharmaceutical samples of TRB HCl (Lamifen tablets) produced by Jamjoom Pharmaceutical Industries (KSA) were purchased from a local provider.

2.3. Blood plasma sample preparation

A healthy volunteer provided drug-free human blood plasma samples. The plasma sample was kept at 37°C for 5 min. After adding 2 mL of methanol, the mixture was centrifuged for 5 min at 3000 rpm. The deproteinized human serum was diluted to 20 mL by doubly distilled water [43]. Working samples were prepared by spiking with concentrations of 5, 30, and 50 $mg.L^{-1}$ TRB HCl to attain suitable concentrations in plasma, and the acidity was adjusted to a pH of 8.5.

A blank solution containing all ingredients except the drug was analyzed simultaneously using the same procedure. The drug content was derived from the corresponding regression equation.

2.4. Procedures for tablets

The contents of 5 tablets were weighed accurately and powdered. Tablets equivalent to 6.45 mg of TRB HCl were transferred into a 25 mL volumetric flask, and 15 mL of methanol were added. The mixture was sonicated for 20 min, and filtered into a 100 mL volumetric flask, and then the volume was completed with distilled water. The solution was filtered through Whatman filter paper (0.45µm) to obtain the working

solution of 65 µg. mL^{-1} concentration. This extract was further diluted with distilled water. The nominal content was calculated either from a calibration curve or using the corresponding regression equation [44].

2.5. General procedures

2.5.1. Preparation of PUF

A mass of 5 g of PUF was cut into uniform shapes (1 cm × 1 cm × 3 mm). The PUF pieces were washed with acetone and deionized water. The PUF pieces were then allowed to dry at room temperature, and then they were soaked in 50 mL of 6 M HCl with continuous stirring for 120 min. Finally, the PUF pieces were washed with deionized water and allowed to dry again at room temperature.

2.5.2. Batch technique

The removal of TRB HCl was carried out using the batch technique at room temperature. 0.1g of either CS or PUF was mixed with 25 mL TRB HCl (40 ppm) and shaken for 30 min at 250 rpm. The CS and PUF containing the adsorbed TRB HCl were filtered, and the residual amounts of drug were spectrophotometrically measured at the λ_{max} of TRB HCl (282 nm). The percentage of removal was calculated using **Eq. 1.**

$$R\% = 100 \times (C_o - C_t)/C_o \qquad \textbf{Eq. 1}$$

Where C_o is the initial concentration and C_t is the final concentration of adsorbate in the liquid phase ($mg.L^{-1}$) [45].

The effect of pH on the removal of TRB HCl was examined within the pH range of 3.6 to 11.0 by adding 0.1 g of either CS or PUF to12.5 mL of TRB HCl (40 ppm) and 2.5 mL of each buffer and shaking for 30 min. The absorbance of samples was measured against a drug-free blank at λ_{max} of the drug.

The influence of extraction time on sorption capacity was investigated at different time intervals (0-100 min) at 250 rpm with adjusting the optimal pH of maximum extraction. The effect of sorbent's amount on the removal of TRB HCl from aqueous media was studied by adding (0.05-1.5 g) CS or PUF to 12.5 ml TRB HCl solution of 40 ppm, with shaking for 30 min after adjusting the optimal pH at room temperature. The remaining TRB HCl in the solution was determined.

Furthermore, the maximum adsorption capacity of CS and PUF was determined under the same batch conditions by adding variable concentrations of TRB HCl (10-100 ppm). To study the effect of the adsorbent recycling; 0.1 g of either CS or PUF was added to 12.5 mL of TRB HCl (40 ppm) with 2.5 of buffer at the optimum pH value of 8.5 with 10 mL deionized water and shaken for 30 min at 250 rpm. The concentration of the residual TRB HCl was then determined. The CS or PUF were rinsed several times using deionized water, and the same procedures were repeated for each sorbent. Finally, the surface morphology of CS and PUF were characterized using the scanning electron microscope (SEM) at an accelerating voltage of 15 kV.

2.6. Determination of zero-point charge of the sorbents

Potentiometric titration method [46,47] was used to determine the zero-point charge of both CS and PUF sorbents. A mass of 0.01 g of sorbents was added to 20 mL of different buffer solutions and shaken for 4 h at 150 rpm until the pH became constant. The pH of the suspensions was measured using a digital pH meter. The equilibrium pH (ΔpH) was plotted against initial pH values to obtain the potentiometric curves. The pHpzc was identified as the pH where the minimum ΔpH value was obtained [47].

2.7. Computational method: In-silico predictive study

Terbinafine hydrochloride was gauged for its forecasted aquatic toxicity by employing the admetSAR server:
(http://lmmd.ecust.edu.cn/admetsar).

3. Results and Discussion

3.1. Characterizations of Sorbents

3.1.1. Scanning electron microscopy (SEM) characterization

The morphology of the PUF and CS was examined by scanning electron microscopy (SEM) before and after adsorption, as shown in Figure 1. It could be seen that the CS and PUF were irregular with rough texture surfaces and the pores' structures were not homogeneous. Chitosan exhibited a rough membrane-like morphology [48] as shown in Figure 1(A). After adsorption, it was clear that the drug (light area) adhered to the chitosan surface, Figure 1(B). At the same time, PUF had an open-cell structure, as shown in Figure 1(C), where the adsorbate particles can freely circulate between the cells since they are interconnected to each other [49]. After adsorption, the drug is accumulated on the inner surface of the porous structure, as shown in Figure 1(D). The surface area of both adsorbents, as measured by BET was 197 $m^2.g^{-1}$ for PUF and 2 $m^2.g^{-1}$ for CS. These values are matching with the SEM images of both sorbents.

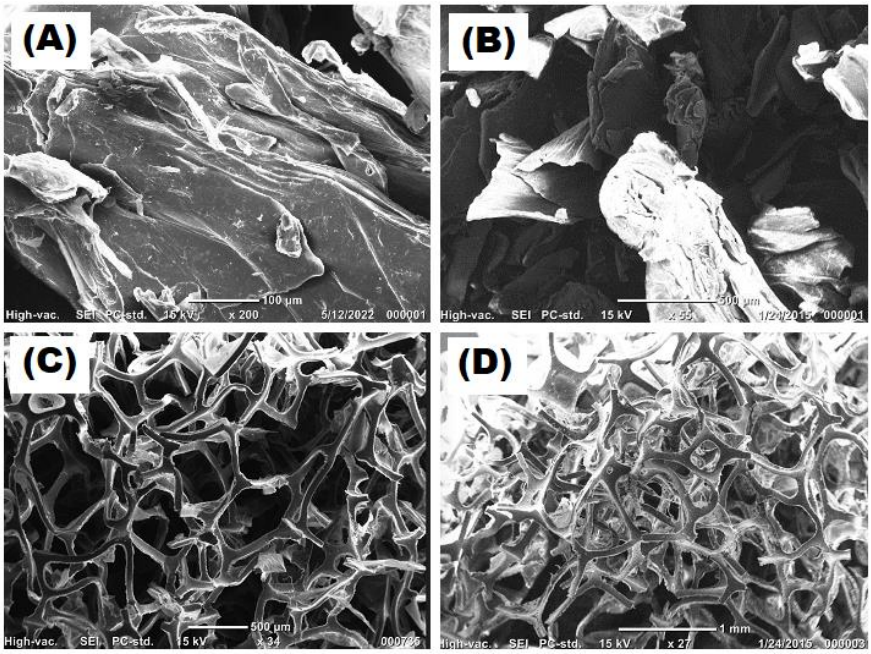

Figure 1. SEM images of (A) CS before adsorption and (B) CS after adsorption of TRB HCl, (C) PUF before adsorption, and (D) PUF after adsorption of TRB HCl

3.1.2. Fourier transform-infrared (FT-IR) spectroscopic characterization

The FT-IR spectra of CS and CS loaded with TRB HCl were observed in the region between 400 and 4000 cm^{-1} (Figure 2).

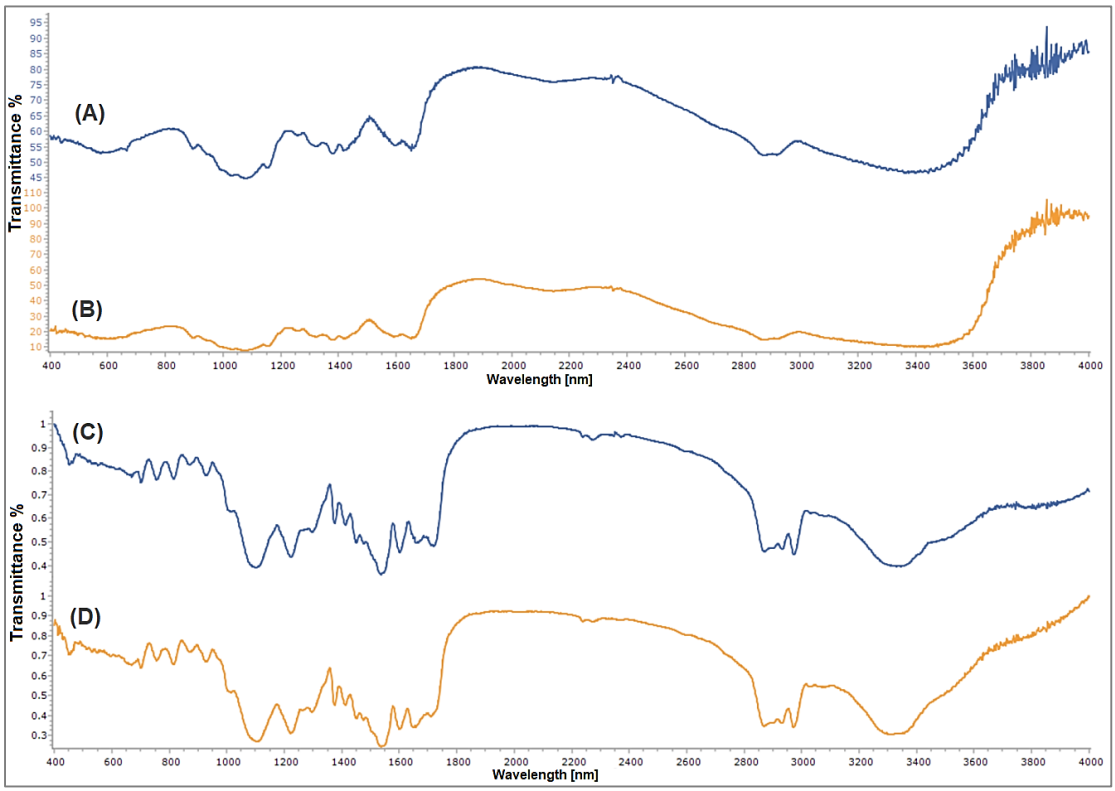

Figure 2. The FT-IR spectra for (A) CS, (B) CS loaded with TRB HCl, (C) PUF and (D) PUF loaded with TRB HCl

In CS spectra, the peaks at 680, 1090, 1430 cm^{-1} indicate NH out-of-plane, C-O, and C-CH_2, respectively. The bands at 1430 & 1450 cm^{-1} correspond to the $-CH_2COOH$ group. The spectrum also shows some peaks near 1590 & 1650 cm^{-1} for the C=O group of the acetyl groups. The band at 2920 cm^{-1} corresponds to NH_2 stretch of amide groups

& CH_2 stretch. Broad peaks, OH bonding groups, and $-NH_3^+$ appear at 3500 - 3200 cm^{-1}.

The NH_2 stretching of primary amine occurs at 3500 - 3300 cm^{-1} [50]. Figure 2 shows the FT-IR spectra of PUF **(C)** and PUF loaded with TRB HCl **(D)**. In PUF, the symmetric and asymmetric N–H Stretching occurs at 3300, and 3350 cm^{-1}, and the medium strong peak near 1530 cm^{-1} indicates NH in-plane. C=O Stretching esters and asymmetric stretching vibration of C–O (from N–CO–O) appear at 1730 and 1230 cm^{-1}, respectively. The 930 cm^{-1} peak indicates N–CO–O symmetric stretching. The C=C in the benzene ring appears at 1605 cm^{-1}, and the weak peaks at 760 - 910 cm^{-1} are typical for out-of-plane bending vibration of C–H in multi-substituted benzene ring [51].

3.1.3. X-ray diffraction (XRD) analysis

XRD analysis was used to determine the state of dispersion of TRB HCl in CS and PUF structures.

XRD diffraction of the CS and CS loaded with TRB HCl are shown in Figures 3(A) and (B), respectively.

CS crystal structure has a broad peak at $2\theta = 20°$ [52], while CS loaded with TRB HCl has shown a decrease in the intensity of the peak at $2\theta = 20°$.

The PUF has a broad diffraction peak observed at $2\theta = 20°$, which indicates the amorphous properties of PUF [53], it also records peaks at $2\theta = 26°$, 44°, and 50°.

The PUF loaded with TRB HCl, Figure 3(D), has shown a decrease in the peak intensity at $2\theta = 20°$ and 50° compared with PUF, Figure 3(C).

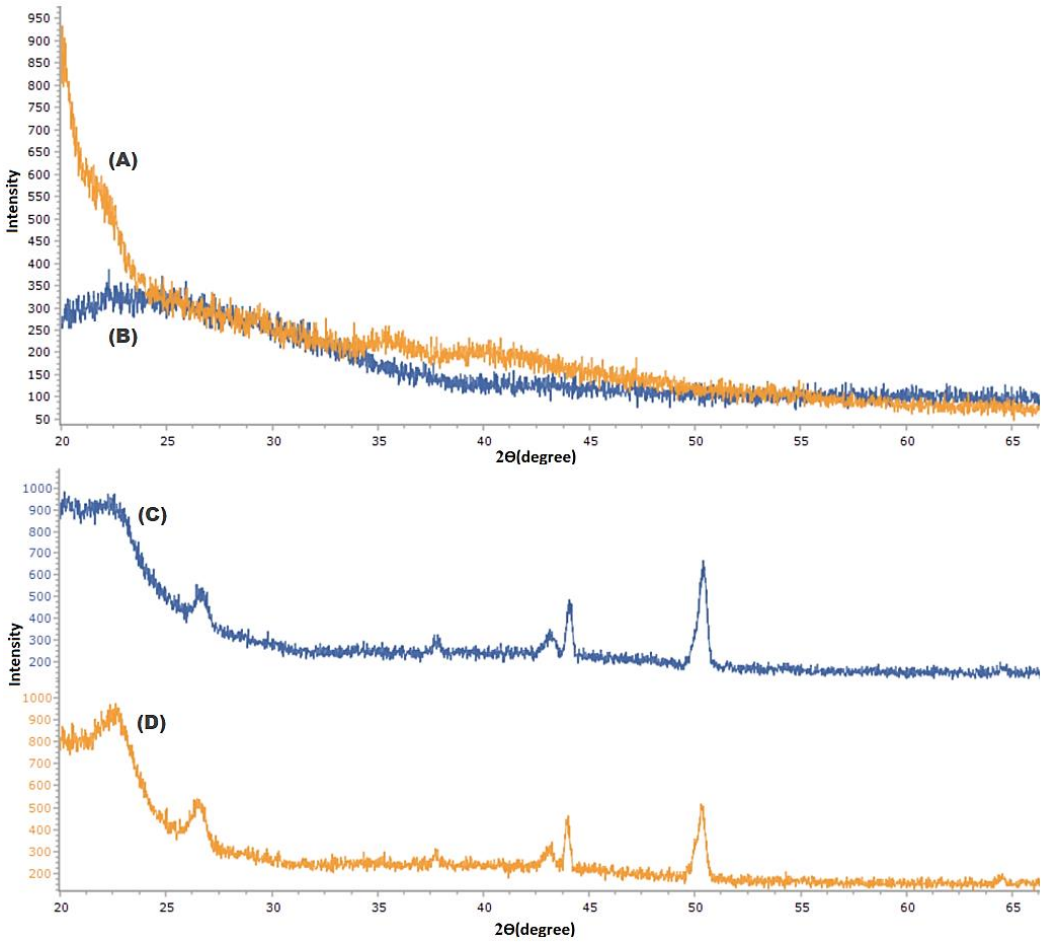

Figure 3. The XRD analysis for (A) CS loaded with TRB HCl, (B) CS, (C) PUF, and (D) PUF loaded with TRB HCl

3.2. Determination of Zero-Point Charge (pHpzc)

To obtain information about the charged surface of CS and PUF, a zero-point charge (pHpzc) was determined. ΔpH was measured and plotted versus the initial pH, and the results are shown in Figure 4.

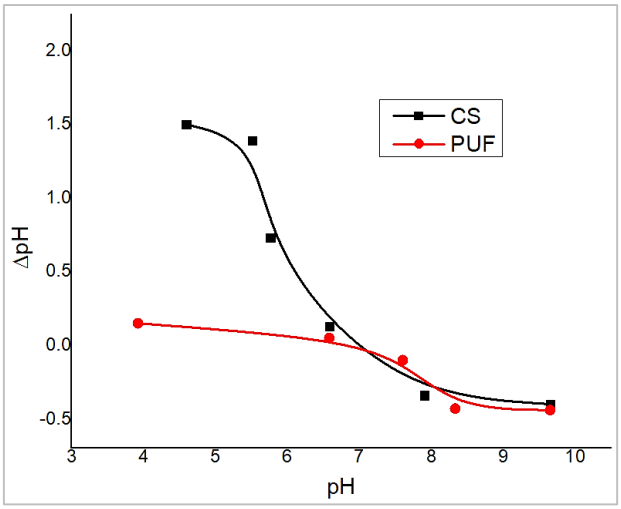

Figure 4. Zero-point charge of CS and PUF

The pH_{ZPC} values of CS and PUF surfaces were 6.8 and 7, respectively [47,54]. The sorbents will be negatively charged at pH above zero-point charge and positively charged at pH's below it [55]. The maximum removal of TRB HCl onto CS and PUF happens at pH's above the pHzpc. So, it is estimated that the sorbent's surface becomes negatively charged and attracts cations drug from the solution. Figure 5 represents a suggested mechanism of electrostatic attraction of TRB with chitosan and PUF [47].

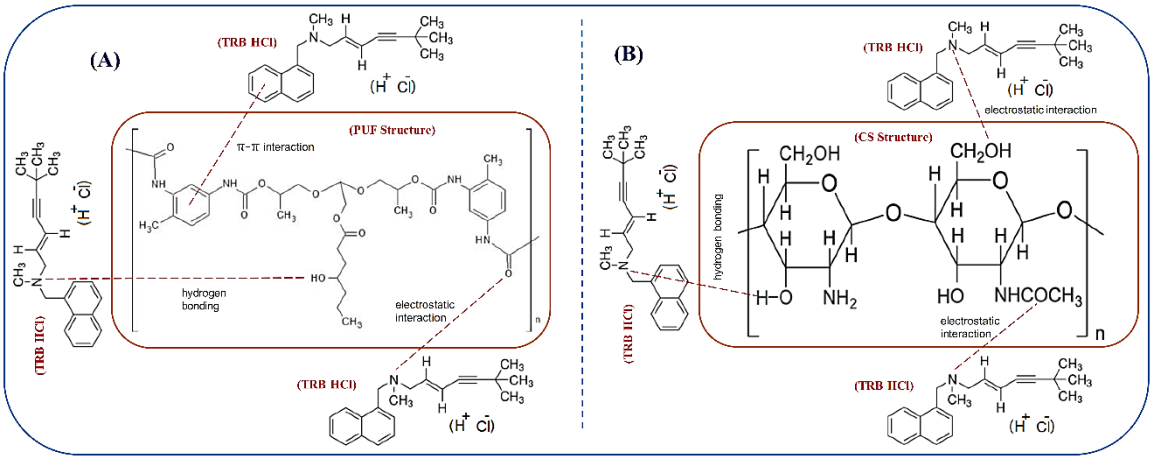

Figure 5. A schematic representation of the suggested adsorption mechanism for TRB HCl by (A) PUF and (B) CS

3.3. Effect of pH

The pH plays a vital role in deciding the adsorbent's maximum adsorption capacity because it significantly controls the adsorbate's removal mechanism and influences the adsorbent's adsorption sites [56]. The effect of pH on the sorption of TRB HCl onto CS and PUF was studied using the batch technique. The different pH values were plotted against the removal percentage, as shown in Figure 6(A). The results have shown that the removal of TRB HCl by both CS and PUF increases with increasing the pH. At low pH, competition from hydronium ions may result in a significant reduction in TRB HCl adsorption. In addition, the solubility of the drug itself can be influenced by changing the pH (from acid to neutral), which leads to an increase in the adsorption affinity for the sorbent surface. Moreover, the increased removal of the drug with the increase in the pH of the solution could be attributed to possible changes in the surface properties [57]. In the case of PUF, hydrogen bonds formed between nitrogen atoms present on TRB HCl and urethane's NH, terminal NH_2, ether oxygen [CH_2–O–CH_2], and OH groups in PUF. At lower pH, nitrogen and oxygen atoms of the PUF tend to be protonated, which makes them unable to bond to TRB HCl molecules [43]. Chitosan has a positive charge; it is protonated at pHs below 6.5 [58], so the lower the pH value is, the more positive charges chitosan carries [59] as the repulsion forces with cationic TRB ions may lower the absorption capacity. The optimum pH to separate TRB HCl from aqueous media by CS and PUF from aqueous solution was 8.5. In a previous study by Abbasi L. et al. [60] on removing TRB HCl from sodium dodecyl sulfate-coated Fe_3O_4 nanoparticles, the optimum adsorption was achieved at a pH of 2.0.

3.4. Effect of Contact Time

Figure 6(B) shows the adsorbed quantity of TRB HCl ($mg.g^{-1}$) at various contact periods for CS and PUF sorbents. The adsorption increased with increasing the time of shaking from 0 to 60 min, then gradually decreased for CS till 100 min, while for PUF, it remained almost constant. Although the adsorbed quantity was higher at the beginning because a large number of active sites was still available on the sorbent's surface, over time, the number of those active sites is reduced, and no further adsorption takes place [61-63]. These results indicate that the optimum exposure period is 60 min for the removal by both sorbents. In a previous study on removing TRB HCl using sodium dodecylsulfate-coated Fe_3O_4 nanoparticles [60], a period of 1 min was found to be an optimal sorption time.

3.5. Effect of Sorbents Amount

The effect of removal of TRB HCl (40 ppm) as a function of the dosage of both sorbents is shown in Figure 6(C). At very high amounts of CS biosorbents; the sorption capacity has shown a decreasing trend due to the comparatively lower concentration of TRB HCl and a large number of the available active sites on the sorbent's surface [64,65]. While in the case of PUF, it was apparent that by increasing the PUF dose, the removal rises to up to 0.4 g in 12.5 mL TRB HCl solution. The presence of a high amount of the sorbents increases the availability of active sites and therefore promotes more excellent removal of TRB HCl from the aqueous medium. Increasing the amount of the sorbent above a certain amount can cause an accumulation of the sorbent's pieces. This, in turn, can quickly reduce their exposed surface area, blocking the active sites from binding to TRB HCl particles [63]. The optimal removal was reached at 0.4 g for both sorbents in 12.5 mL TRB HCl.

3.6. Effect of Drug Capacity

The effect of the initial concentration of the TRB HCl is essential for the sorption capacity and hence, for sorption effectiveness [66]. The removal percentage at different concentrations of TRB HCl (10-100 ppm) are shown in Figure 6(D). CS has demonstrated a decrease in the removal percentage by increasing the concentration of the TRB HCl solution. This might be attributed to the low ratio of the initial number of adsorbate drug particles to the available surface area at a lower concentration. In contrast, at high concentrations, the available adsorption sites become fewer. The increase in the percentage of removal by PUF with an increase in the TRB HCl concentration was attributed to the high initial concentration of TRB HCl, which accelerates the driving force and reduces the resistance to mass transfer. Therefore, increasing the initial TRB HCl concentration also improves the interaction between the adsorbent and the TRB HCl particles in the aqueous solution [67]. The results of both sorbents indicate that the adsorption depends strongly on the initial concentration of the drug. The maximum removal of TRB HCl was achieved at 20 and 100 ppm concentrations of TRB HCl by CS and PUF, respectively. In a previous study on removing TRB HCl using sodium dodecylsulfate-coated Fe_3O_4 nanoparticles [60], the calibration curve was linear within the range of 0.0025 to 0.5 ppm.

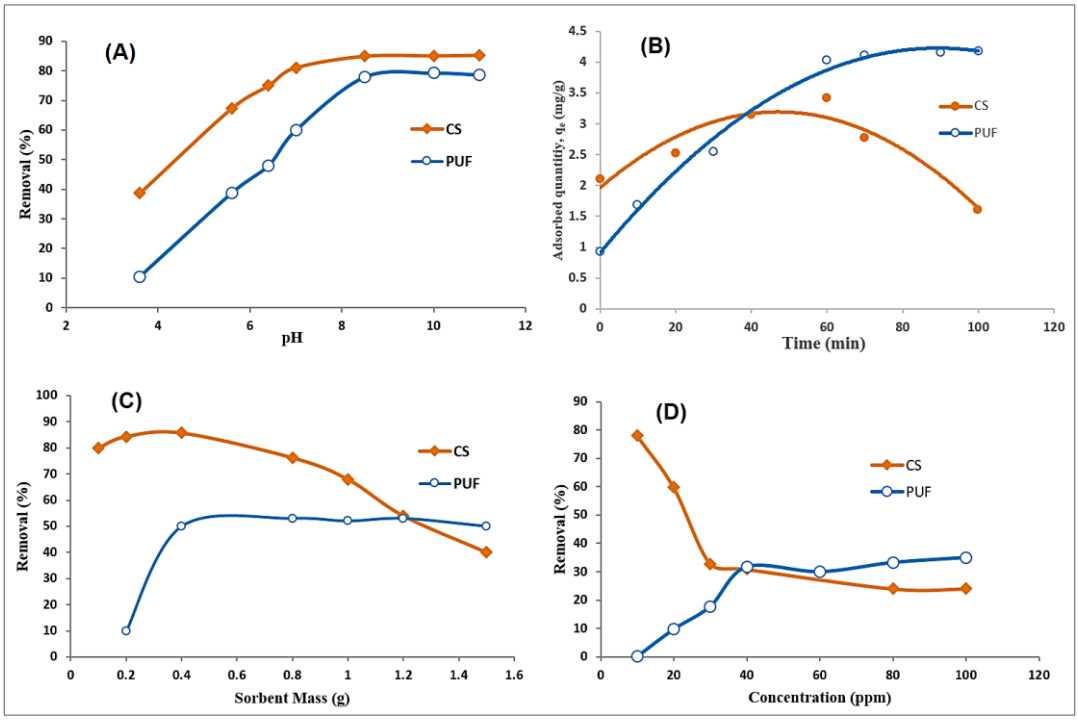

Figure 6. The effect of: (A) pH, (B) contact time period, (C) dosage of sorbents, and (D) initial concentration of TRB HCl

3.7. Reusability of Sorbents

Reusability is one of the essential factors in assessing the effectiveness of sorbents. Therefore, the CS and PUF to re-adsorb the TRB HCl was examined by repeating the experiment under the same ideal conditions until reaching the maximum adsorption limits. The results have shown that they are stable until up to seven cycles of drug adsorption/desorption without noticeable degradation in their sorption capacities. However, after seven cycles, both sorbents have shown a decrease in the TRB HCl removal percentage, probably due to the decreased availability of active adsorption sites.

3.8. Kinetic Studies

The adsorption rate of TRB from the aqueous phase using CS and PUF can be clarified using the pseudo-first-order, pseudo-second-order, Elovich, and intraparticle diffusion kinetic models.

3.8.1. Pseudo-first-order and pseudo-second-order kinetic models

The kinetic models of pseudo-first-order and pseudo-second-order can be represented by **Eq. 2** and **3** [68,69]

$$\ln (q_e - q_t) = \ln q_e - k_1 t \qquad \textbf{Eq. 2}$$

Where q_t and q_e represent the sorption capacity at any time t and its value at equilibrium (mg.g^{-1}), respectively, and k_1 (min^{-1}) is the pseudo-first-order rate constant of the sorption.

$$t/q_t = 1/k_2 q_e^2 + t/q_e \qquad \textbf{Eq. 3}$$

Where k_2 is the rate constant of pseudo-second order adsorption [g.(mg.min)$^{-1}$]. By plotting t/q_t vs. t, the values of k_2 and q_e were estimated.

The pseudo-first-order kinetic model reflects the physisorption process, which depends on vacant sites. The requirement that theoretically calculates equilibrium adsorption capacity (q_e theoretical) should agree with the experimental adsorption capacity (q_e experimental) values [70].

Figure 7(A) shows an agreement between the experimental data and the pseudo-first-order model outputs for TRB HCl adsorption onto both CS and PUF. As shown in Table 1, the correlation coefficients (R^2) are relatively very high (0.966, 0.994) for CS and PUF, respectively, and there is a relatively good agreement between q_e (theoretical) and q_e (experimental).

However, in the pseudo-second-order model, as in Figure 7(B), there is no good agreement between the calculated and experimental values of q_e. This indicates poor fitting with the pseudo-second-order kinetic model. From the findings, it can be concluded that the pseudo-first-order correlation coefficient is higher when compared to the pseudo-second-order, suggesting that the adsorption of TRB HCl on CS and PUF does not follow a pseudo-second-order type of reaction kinetics. The kinetic parameters and the correlation coefficients (R^2) are listed in Table 1. In which the correlation coefficient R^2 = 0.894, 0.919 for CS and PUF, respectively.

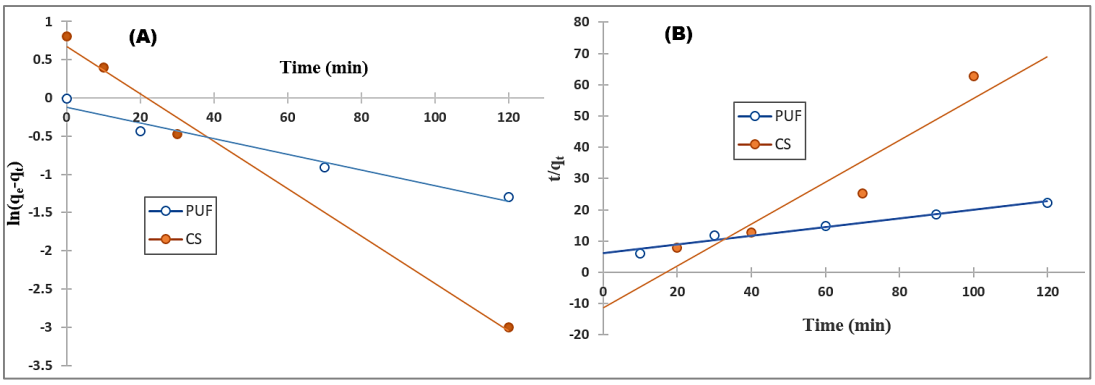

Figure 7. (A) Pseudo first-order and (B) Pseudo second-order kinetic models

3.8.2. Elovich kinetic model

Elovich kinetic model is used to describe chemisorption from Elovich **Eq. 4** [71]:

$$q_t = (1/\beta) \ln(\alpha\beta) + (1/\beta) \ln t \qquad \textbf{Eq. 4}$$

Where α is the initial adsorption rate (mg.g^{-1}.min), and β is the desorption constant (g.mg^{-1}) The parameters of the Elovich equation were estimated by plotting q_t vs. ln t (Figure 8) and are summarized in Table 1. The R-value for PUF is relatively less than the results obtained from pseudo-first- and second-order kinetics. On the other hand, in the case of CS, the R value is somewhat higher than the results obtained from both pseudo-first- and second-order kinetic models. This indicates that the adsorption process obeys Elovich kinetic model, suggesting that the adsorption process could probably be chemisorption corresponding to the heterogeneous nature of the active sites.

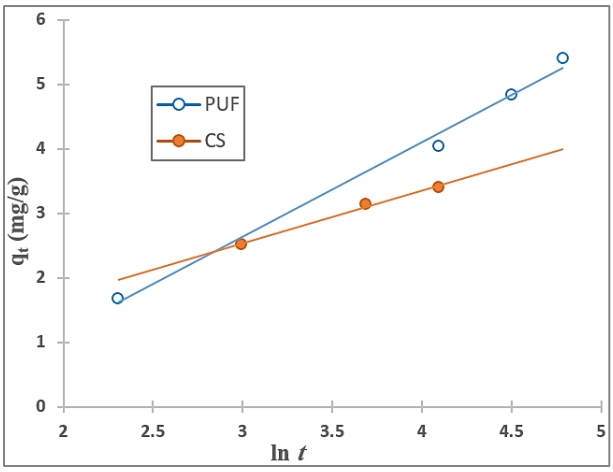

Figure 8. Elovich kinetic model for the adsorption of TRB HCl by CS and PUF

3.8.3. Intraparticle diffusion kinetic model

The intraparticle diffusion kinetic model is represented by **Eq. 5** [72]:

$$q_t = K_p t^{1/2} + C \qquad \textbf{Eq. 5}$$

Where *p* is the intraparticle diffusion rate constant ($mg.g^{-1}.min^{-½}$), *C* is the intercept of the plot, and *K* indicates the boundary layer effect. A larger intercept indicates a more significant contribution of surface sorption in the rate-controlling step. The linear regression plots of *t* vs. $t_{1/2}$ are obtained under the optimum condition for TRB HCl sorption onto CS and PUF. Figure 9 reveals that internal diffusion has not become the rate-limiting step. This deviation in linear regression reflects the existence of some boundary layer effect [71]. Table 1 shows the values of the estimated diffusion parameters.

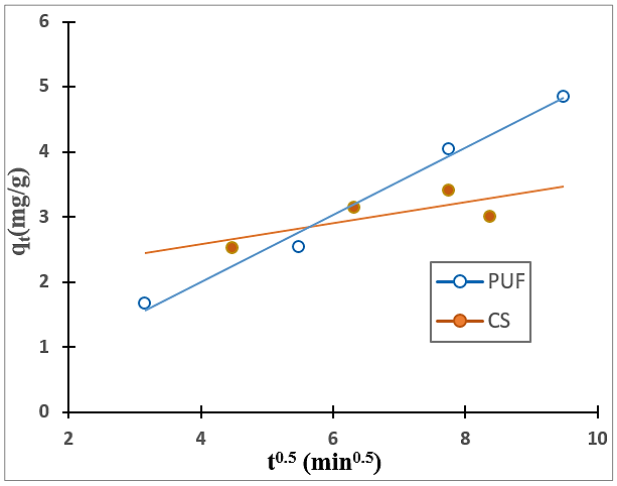

Figure 9. Intraparticle diffusion model fitted to the adsorption data of TRB HCl by CS and PUF

Table 1. The kinetic parameters and the correlation coefficients of pseudo-first-order, pseudo-second-order, Elovich, and intraparticle diffusion models.

Sorbents	q_e *(calc)*	Pseudo-first-order			Pseudo-second-order		
		q_e ($mg.g^{-1}$)	k_1 (min^{-1})	R^2	q_e ($mg.g^{-1}$)	k_2 ($g/mg.min^{-1}$)	R^2
CS	0.991	1.339	0.0235	0.966	1.705	0.065	0.895
PUF	3.169	4.741	0.0716	0.994	5.995	0.008	0.919

To be continued	Elovich model			Intraparticle diffusion		
	α (mg/g/min)	**β** (g.mg^{-1})	R^2	$K^{0.5}$ (mg/(g	**C**	R^2
CS	0.8115	1.223	0.993	0.1596	1.9476	0.5493
PUF	0.1531	0.682	0.991	0.5169	0.0681	0.9885

3.9. Adsorption Isotherm

Modeling the adsorption isotherm data is an essential method of predicting and comparing adsorption performance, which is fundamental for optimizing the adsorption mechanism pathways, expressing adsorbents capabilities, and efficiently designing the adsorption systems.

Langmuir adsorption isotherms were initially developed to describe gas-solid phase adsorption. However, it has also been widely used for other phase systems. This theory relates to homogeneous adsorption, and the empirical model assumes that the adsorption takes place only in a monolayer that has no interaction between the adsorbed molecules [73]. The linear form of the Langmuir isotherm can be represented by **Eq. 6**.

$$C_e/q_e = 1/q_m b + (1/q_m)C_e \qquad \textbf{Eq. 6}$$

Therefore, the plot of C_e/q_e versus C_e gives a straight line with a slope equal to $1/q_m$ and intercept equal to $1/q_m b$.

The linear correlation coefficients for the CS and PUF sorbents were 0.9821 and 0.9228, respectively. The values for q_m and b were 1.229 mg.g^{-1} and 0.1285 L.mg^{-1} for CS, and 2.807 mg.g^{-1} and 0.16035 L.mg^{-1} for PUF, respectively.

Langmuir model shown in Figure 10(A) was obtained by plotting C_e/q_e against C_e, and the empirical parameters of the linear equation are represented in Table 2.

The Freundlich model does not limit adsorption to the formation of monolayers and is often used to describe heterogeneous surfaces [73]. The linear form of the Freundlich isotherm is expressed by **Eq. 7**:

$$\log q_e = \log K_f + (1/n)\log C_e \qquad \textbf{Eq. 7}$$

Where C_e (mg.L^{-1}) and q_e (mg.g^{-1}) are the liquid-phase concentration and the amount of adsorption of adsorbate at equilibrium, respectively. K_f (L^{-1}.mg) and n are the Freundlich constants. Freundlich model was obtained by plotting log q_e against log C_e, as shown in Figure 10(B). The linear correlation coefficients for the CS and PUF sorbents were 0.9777 and 0.9794, respectively. All empirical parameters of the linear equation are represented in Table 2. Based on the linear correlation coefficient (R2) value, the Langmuir model can describe sorption by CS, while the Freundlich model can explain PUF.

Table 2. Adsorption parameters of Langmuir and Freundlich isotherm models.

Sorbent	Langmuir Isotherm				Freundlich Isotherm			
	q_m (mg.g^{-1})	b (L.mg^{-1})	R^2	*RMSE*	K_f (L^{-1}.mg)	n	R^2	*RMSE*
CS	1.2297	0.1285	0.9821	2.3916	0.30255	1.51469	0.9777	0.0859
PUF	2.807	0.16035	0.9228	1.8471	0.52161	0.48281	0.9794	0.0634

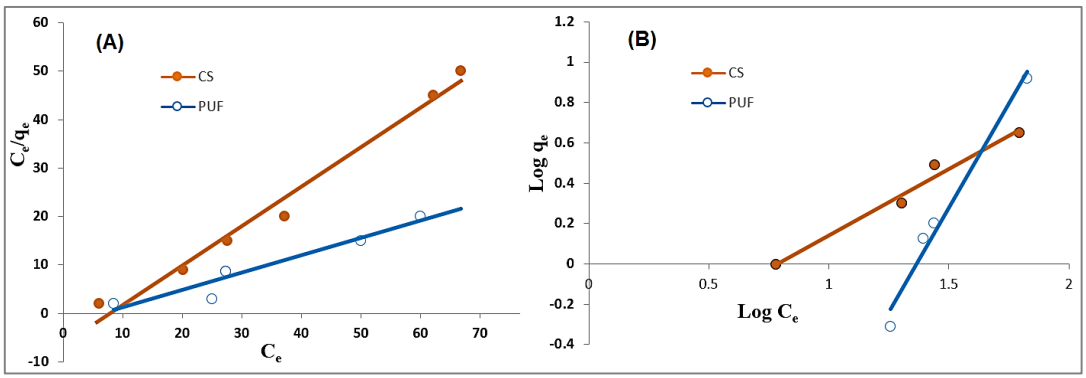

Figure 10. (A) Langmuir isotherm model and, (B) Freundlich isotherm model

3.10. Analysis of the Pharmaceutical Formulations
The proposed method has been successfully used to determine TRB HCl in its commercial tablet form. The results have shown excellent recovery percentages, as summarized in Table 3.

Table 3. Recovery percentages of TRB HCl in its pharmaceutical formulations tablets using CS and PUF.

Sorbents	Taken ($\mu g.mL^{-1}$)	Found[a] ($\mu g.mL^{-1}$)	Recovery (%)	RE[b]
CS	32	31.12	97.25	0.0275
PUF	32	31.5	98.437	0.015625

a: mean value of five determinations

b: relative error

3.11. Application on Spiked Human Blood plasma
The applicability of the proposed was validated for application in a more complex natural matrix, human blood plasma. The fresh blood plasma samples were spiked with TRB HCl at concentration levels of 5, 30, 50 $mg.L^{-1}$ to validate the suitability of both CS and PUF sorbents in such a complex medium. The results are shown in Figure 11 and summarized in Table 4.

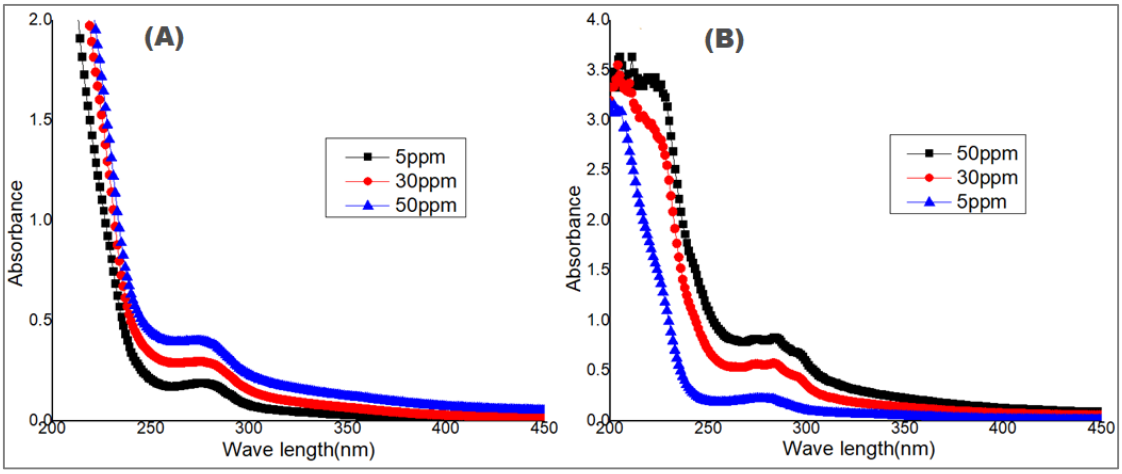

Figure 11. The validation of the method using (A) CS and (B) PUF sorbents for the elimination of TRB HCl from human blood plasma

Table 4. The elimination of TRB HCl from human blood plasma using CS and PUF sorbents (method validation).

Sorbents	Spiked ($\mu g.mL^{-1}$)	Found[a] ($\mu g.mL$-1)	Recovery (%)	RE[b]
PUF	5	4.585	91.7	0.415
	30	29.53	98.43	0.47
	50	49.82	99.6	0.18
CS	5	4.21	84.2	0.79
	30	28.65	95.5	1.35
	50	49.0	98.0	1.0

a: mean value of five determinations
b: relative error

3.12. Comparison with other Methods
The efficiency of removal (%) of TRB HCl by both CS and PUF sorbents has been compared to that of other sorbents reported by previous studies, as summarized in Table 5.

Table 5. Comparison of Removal efficiency of TRB HCl.

Method	Detection Technique	Media	Sorbent	Removal efficiency%	Reference
Extraction	HPLC-UV[a]	Water Urine Plasma	Fe_3O_4 NPs[b]	67 58 26	[60]
Sorption	Spectrophotometric	Water	βCD[c]	92	[74]
Sorption	Spectrophotometric	Water	CS PUF	78 35	This work
		Plasma	CS PUF	97.25 98.437	

[a] high-performance liquid chromatography with ultraviolet/visible detector,
[b] Fe_3O_4 nanoparticles,
[c] β-cyclodextrin.

3.13. In-silico Aquatic Toxicity Computational Predictions

The work investigated here was done with the intent to remove TRB HCl from aqueous solutions, so it was worthy of forecasting the aquatic toxicity of TRB HCl. Terbinafine hydrochloride (TRB HCl) has been reported as a highly toxic pollutant for aquatic life. Its forecasted fish toxicity is 0.1360 (pLC50, $mg.L^{-1}$), while that of tetrahymena pyriformis (the selected toxic endpoint) is 1.1784 (pIGC50, $\mu g.L^{-1}$). TRB HCl emerged as a not-ready biodegradable compound, with high FHTM (fathead minnow toxicity) and high TPT (tetrahymena pyriformis toxicity) in the predictive computational studies.

4. Conclusion

The removal of Terbinafine Hydrochloride (TRB HCl) antifungal drug contaminant from aqueous media using chitosan (CS) and polyurethane foam (PUF) has proven to be an effective, simple, yet low-cost alternative technique for possible decontamination applications of aquatic systems as well as complex biological media. Both sorbents have successfully removed the TRB HCl drug ions from the aqueous medium with optimal removal percentages of 78 and 35 for CS and PUF, respectively, at optimum operating conditions of a pH = 8.5, sorbent's amount of 0.4 g in 12.5 mL TRB HCl (40 ppm), and a maximum contact period of 60 min. The results have been confirmed using SEM, FT-IR, and XRD characterizations. By determining the zero-point charge (pHpzc) for the studied sorbents, it was obvious that electrostatic attraction is one of the mechanisms in TRB HCl sorption. The kinetic studies have shown that the adsorption of TRB HCl on CS and PUF does follow a pseudo-first-order type of reaction kinetics. Langmuir adsorption isotherm model indicates that the maximum sorption capacities were 1.2297 and 2.807 $mg.g^{-1}$ for CS and PUF, respectively. Based on the linear correlation coefficient (R2) value, the Langmuir model can describe sorption by CS, while the Freundlich model can describe PUF. The proposed method was validated by using CS and PUF to remove TRB HCl from spiked blood plasma as an example of a complex medium. TRB HCl was explored for its aquatic toxicity utilizing *in-silico* computational predictions.

It became highly toxic for aquatic life, making its removal from aquatic systems a high environmental priority.

Acknowledgments

This work was funded and supported by the Deputyship for Research & Innovation, Ministry of Education of Saudi Arabia, through project 442/16.

The authors extend their appreciation to Taibah University for its supervision support. In addition, the authors thank Mrs. Ghena Saud for her valuable assistance in data acquisitions.

References

1- G. Crini, E. Lichtfouse, Wastewater treatment: an overview, *Green adsorbents for pollutant removal*, **2018**, 1-21.
2- P. M. Pakdel, S. J. Peighambardoust, Review on recent progress in chitosan-based hydrogels for wastewater treatment application, *Carbohydrate Polymers*, **2018**, 201, 264-279.
3- S. Mudgal, A. De Toni, S. Lockwood, K. Salès, T. Backhaus, B. H. Sorensen, Study on the environmental risks of medicinal products: Final Report prepared by BIO Intelligent Service, *Executive Agency for Health and Consumers*, **2013**.
4- M. Sousa, C. Gonçalves, V. J. Vilar, R. A. Boaventura, M. Alpendurada, Suspended TiO2-assisted photocatalytic degradation of emerging contaminants in a municipal WWTP effluent using a solar pilot plant with CPCs, *Chemical Engineering Journal*, **2012**, 198, 301-309.
5- M. Patel, R. Kumar, K. Kishor, T. Mlsna, C. U. Pittman Jr, D. Mohan, Pharmaceuticals of emerging concern in aquatic systems: chemistry, occurrence, effects, and removal methods, *Chemical Reviews*, **2019**, 119, 3510-3673.
6- R. Mrutyunjayarao, S. Naresh, K. Pendem, P. R. Rao, C. Sasttry, U. V. Prasad, Three simple spectrometric determination of terbinafine hydrochloride (TRB) in pure state and tablets,

Proceedings of the National Academy of Sciences, *India Section A: Physical Sciences*, **2012**, 82, 221-224.
7- B. Kanakapura, V. K. Penmatsa, Analytical methods for determination of terbinafine hydrochloride in pharmaceuticals and biological materials, *Journal of Pharmaceutical Analysis*, **2016**, 6, 137-149.
8- British pharmacopoeia, https://www.pharmacopoeia.com. **2016**, 15 Sept 2020.
9- J. Fick, H. Söderström, R. H. Lindberg, C. Phan, M. Tysklind, D. J. Larsson, Contamination of surface, ground, and drinking water from pharmaceutical production, *Environmental Toxicology and Chemistry*, **2009**, 28, 2522-2527.
10- S. G. Cardoso, E. E. Schapoval, UV spectrophotometry and nonaqueous determination of terbinafine hydrochloride in dosage forms, *Journal of AOAC International*, **1999**, 82, 830-833.
11- K. Patel, V. Karkhanis, A validated HPTLC method for determination of Terbinafine hydrochloride in pharmaceutical solid dosage form, *International Journal of Pharmaceutical Sciences*, **2012**, 3, 4492-4495.
12- J. Denouël, H. Keller, P. Schaub, C. Delaborde, H. Humbert, Determination of terbinafine and its desmethyl metabolite in human plasma by high-performance liquid chromatography, *Journal of Chromatography B: Biomedical Sciences Applications*, **1995**, 663, 353-359.
13- C. Wang, Y. Mao, D. Wang, G. Yang, Q. Qu, X. Hu, Voltammetric determination of terbinafine in biological fluid at glassy carbon electrode modified by cysteic acid/carbon nanotubes composite film, *Bioelectrochemistry*, **2008**, 72, 107-115.
14- F. Faridbod, M. R. Ganjali, P. Norouzi, Potentiometric PVC membrane sensor for the determination of terbinafine, *International Journal of Electrochemical Science*, **2013**, 8, 6107-6117.
15- M. Chennaiah, T. Veeraiah, T. V. Kumar, G. Venkateshwarlu, Extractive spectrophotometric methods for determination of terbinafine hydrochloride in pharmaceutical formulations using some acidic triphenylmethane dyes, *Indian Journal of Chemical Technology*, **2012**, 19, 218-221.
16- F. Belal, M. S. El-Din, M. Eid, R. El-Gamal, Spectrofluorimetric determination of terbinafine hydrochloride and linezolid in their dosage forms and human plasma, *Journal of fluorescence*, **2013**, 23, 1077-1087.
17- K. Mielech-Łukasiewicz, A. Dąbrowska, Comparison of boron-doped diamond and glassy carbon electrodes for determination of terbinafine in pharmaceuticals using differential pulse and square wave voltammetry, *Analytical Letters*, **2014**, 47, 1697-1711.
18- F. S. Felix, L. M. Ferreira, P. d. O. Rossini, C. L. do Lago, L. Angnes, Quantification of terbinafine in pharmaceutical tablets using capillary electrophoresis with contactless conductivity detection and batch injection analysis with amperometric detection, *Talanta*, **2012**, 101, 220-225.
19- N. Brignol, R. Bakhtiar, L. Dou, T. Majumdar, F. Tse, Quantitative analysis of terbinafine (Lamisil®) in human and minipig plasma by liquid chromatography tandem mass spectrometry, *Rapid communications in mass spectrometry*, **2000**, 14, 141-149.
20- R. Choumane, S. Peulon, Electrodeposited birnessite thin film: An efficient eco-friendly sorbent for removing heavy metals from water, *Colloids Surfaces A: Physicochemical Engineering Aspects*, **2019**, 577, 594-603.
21- A. M. Elgarahy, A. Akhdhar, A. S. Al-Bogami, K. Z. Elwakeel, Magnetically separable solid phase extractor for static anionic dyes adsorption from aqueous solutions, *Surfaces and Interfaces*, **2022**, 30, 101962.
22- A. A. Yakout, M. A. Shaker, K. Z. Elwakeel, W. Alshitari, Response surface methodological optimization of batch Cu (II) sorption onto succinic acid functionalized SiO_2 nanoparticles, *Canadian Journal of Chemistry*, **2019**, 97, 277-286.
23- A. A. Yakout, M. A. Shaker, K. Z. Elwakeel, W. Alshitari, Lauryl sulfate@ magnetic graphene oxide nanosorbent for fast methylene blue recovery from aqueous solutions, *Journal of Dispersion Science and Technology*, **2019**, 40, 707-715.
24- S. Kanamarlapudi, V. K. Chintalpudi, S. Muddada, Application of biosorption for removal of heavy metals from wastewater, *Biosorption*, **2018**, 18, 69.
25- A. Elgarahy, K. Elwakeel, S. Mohammad, G. Elshoubaky, A critical review of biosorption of dyes, heavy metals and metalloids from wastewater as an efficient and green process, *Cleaner Engineering and Technology*, **2021**, 4, 100209.
26- D. Huang, B. Li, J. Ou, W. Xue, J. Li, Z. Li, T. Li, S. Chen, R. Deng, X. Guo, Megamerger of biosorbents and catalytic technologies for the removal of heavy metals from wastewater: Preparation, final disposal, mechanism and influencing factors, *Journal of Environmental Management*, **2020**, 261, 109879.
27- S. Islam, M. A. R. Bhuiyan, M. N. Islam, Chitin and Chitosan: Structure, Properties and Applications in Biomedical Engineering, *Journal of Polymers and the Environment*, **2016**, 25, 854-866.
28- T. Chang, Cell encapsulation technology and therapeutics, *Springer Science & Business Media*, **2013**.
29- M. S. Almughamisi, Z. A. Khan, W. Alshitari,

K. Z. Elwakeel, Recovery of chromium (VI) oxyanions from aqueous solution using Cu (OH) 2 and CuO embedded chitosan adsorbents, *Journal of Polymers and the Environment*, **2020**, 28, 47-60.
30- K. Z. Elwakeel, A. S. Al-Bogami, A. M. Elgarahy, Efficient retention of chromate from industrial wastewater onto a green magnetic polymer based on shrimp peels, *Journal of Polymers and the Environment*, **2018**, 26.
31- S. Wei, Y. C. Ching and C. H. Chuah, Synthesis of chitosan aerogels as promising carriers for drug delivery: A review, *Carbohydrate Polymers*, **2019**, 231, 115744.
32- M. Saraji, M. Tarami, N. Mehrafza, Preparation of a nano-biocomposite film based on halloysite-chitosan as the sorbent for thin film microextraction, *Microchemical Journal*, **2019**, 150, 104171.
33- T. Zidan, A. E. Abdelhamid, E. Zaki, N-Aminorhodanine modified chitosan hydrogel for antibacterial and copper ions removal from aqueous solutions, *International Journal of Biological Macromolecules*, **2020**, 158, 32-42.
34- K. Z. Elwakeel, Environmental application of chitosan resins for the treatment of water and wastewater: a review, *Journal of dispersion science and technology*, **2010**, 31, 273-288.
35- V. Lemos, M. Santos, E. Santos, M. Santos, W. Dos Santos, A. Souza, D. De Jesus, C. Das Virgens, M. Carvalho, N. Oleszczuk, Application of polyurethane foam as a sorbent for trace metal pre-concentration—A review, *Spectrochimica acta part B: Atomic spectroscopy*, **2007**, 62, 4-12.
36- M. S. El-Shahawi, H. Alwael, A novel platform based on gold nanoparticles chemically impregnated polyurethane foam sorbent coupled ion chromatography for selective separation and trace determination of phosphate ions in water, *Microchemical Journal*, **2019**, 149, 103987.
37- H. Li, L. Liu, F. Yang, Hydrophobic modification of polyurethane foam for oil spill cleanup, *Marine Pollution Bulletin*, **2012**, 64, 1648-1653.
38- E. Moawed, N. Burham, M. El-Shahat, Separation and determination of iron and manganese in water using polyhydroxyl polyurethane foam, *Journal of the Association of Arab Universities for Basic and Applied Sciences*, **2013**, 14, 60-66.
39- M. F. Silva, D. Rigo, V. Mossi, R. M. Dallago, P. Henrick, G. de Oliveira Kuhn, C. Dalla Rosa, D. Oliveira, J. V. Oliveira, H. Treichel, Evaluation of enzymatic activity of commercial inulinase from Aspergillus niger immobilized in polyurethane foam, *Food and Bioproducts Processing*, **2013**, 91, 54-59.
40- A. A. Nikkhah, H. Zilouei, A. Asadinezhad, A. Keshavarz, Removal of oil from water using polyurethane foam modified with nanoclay, *Chemical Engineering Journal*, **2015**, 262, 278-285.
41- A. Keshavarz, H. Zilouei, A. Abdolmaleki, A. Asadinezhad, Enhancing oil removal from water by immobilizing multi-wall carbon nanotubes on the surface of polyurethane foam, *Journal of Environmental Management*, **2015**, 157, 279-286.
42- S. Ranote, D. Kumar, S. Kumari, R. Kumar, G. S. Chauhan, V. Joshi, Green synthesis of Moringa oleifera gum-based bifunctional polyurethane foam braced with ash for rapid and efficient dye removal, *Chemical Engineering Journal*, **2019**, 361, 1586-1596.
43- S. M. A. Azeem, S. Ali, M. F. El-Shahat, Sorption characteristics of caffeine onto untreated polyurethane foam: application to its determination in human plasma, *Analytical Sciences*, **2011**, 27, 1133-1133.
44- K. Patel, V. Karkhanis, A validated HPTLC method for determination of Terbinafine hydrochloride in pharmaceutical solid dosage form, *International Journal of Pharmaceutical Sciences and Research*, **2012**, 3, 4492-4495.
45- G. Crini, E. Lichtfouse, L. D. Wilson, N. Morin-Crini, Adsorption-oriented processes using conventional and non-conventional adsorbents for wastewater treatment, *Springer, Cham*, **2018**, 23-71.
46- N. Fiol, I. Villaescusa, Determination of sorbent point zero charge: usefulness in sorption studies, Environmental chemistry letters, **2009**, 7, 79-84.
47- S. Ali, S. M. Sirry, H. A. Hassanin, Removal and characterisation of Pb(II) ions by xylenol orange-loaded chitosan: equilibrium studies, *International Journal of Environmental Analytical Chemistry*, **2020**, 1-13.
48- Y. Luo, Q. J. J. o. F. P. Wang, Beverages, Recent advances of chitosan and its derivatives for novel applications in food science, *Journal of Food Processing & Beverages*, **2013**, 1, 1-13.
49- R. Gómez-Rojo, L. Alameda, Á. Rodríguez, V. Calderón, S. Gutiérrez-González, Characterization of polyurethane foam waste for reuse in eco-efficient building materials, *Polymers*, **2019**, 11, 359-374.
50- Z. Abdeen, S. G. Mohammad, Study of the adsorption efficiency of an eco-friendly carbohydrate polymer for contaminated aqueous solution by organophosphorus pesticide, *Open Journal of Organic Polymer Materials*, **2013**, 2014.
51- L. Jiao, H. Xiao, Q. Wang, J. Sun, Thermal degradation characteristics of rigid polyurethane foam and the volatile products analysis with TG-FTIR-MS, *Polymer Degradation and Stability*, **2013**, 98, 2687-2696.
52- S. Kumar, J. Koh, Physiochemical, optical and biological activity of chitosan-chromone derivative for biomedical applications, *International Journal of Molecular Sciences*, **2012**, 13, 6102-6116.
53- J. Li, J.-L. Gong, G.-M. Zeng, P. Zhang, B. Song, W.-C. Cao, H.-Y. Liu, S.-Y. Huan, Zirconium-based metal organic frameworks loaded on

polyurethane foam membrane for simultaneous removal of dyes with different charges, *Journal of colloid and interface science*, **2018**, 527, 267-279.

54- A. Dong, G. Hou, M. Feng, A. Li, Properties of amphoteric polyurethane waterborne dispersions. III. Isoelectric points and precipitation, *Journal of Polymer Science Part B: Polymer Physics*, **2002**, 40, 2440-2448.

55- M. M. Ibrahim, W. W. Ngah, M. Norliyana, W. W. Daud, M. Rafatullah, O. Sulaiman, R. Hashim, A novel agricultural waste adsorbent for the removal of lead (II) ions from aqueous solutions, *Journal of Hazardous Materials*, **2010**, 182, 377-385.

56- A. Kurniawan, H. Sutiono, N. Indraswati, S. Ismadji, Removal of basic dyes in binary system by adsorption using rarasaponin–bentonite: Revisited of extended Langmuir model, *Chemical Engineering Journal*, **2012**, 189, 264-274.

57- R. A. Al-Bayati, A. S. Ahmed, Adsorption-desorption of trimethoprim antibiotic drug from aqueous solution by two different natural occurring adsorbents, *International Journal of Chemistry*, **2011**, 3, 21-30.

58- M. Thanou, J. Verhoef, H. Junginger, Oral drug absorption enhancement by chitosan and its derivatives, *Advanced Drug Delivery Reviews*, **2001**, 52, 117-126.

59- Y.-C. Chung, Y.-H. Li, C.-C. Chen, Pollutant removal from aquaculture wastewater using the biopolymer chitosan at different molecular weights, *Journal of Environmental Science and Health*, P*art A: Toxic/Hazardous Substances and Environmental Engineering*, **2005**, 40, 1775-1790.

60- L. Abbasi, M. Faraji, M. Bahmaie, Extracting trace amount of terbinafine hydrochloride in biological fluids and wastewater samples using solid-phase-extraction based on magnetic nanoparticles followed by HPLC-UV analysis, *Asia-Pacific Journal of Chemical Engineering*, **2014**, 9, 826-833.

61- V. Oskoei, M. Dehghani, S. Nazmara, B. Heibati, M. Asif, I. Tyagi, S. Agarwal, V. K. Gupta, Removal of humic acid from aqueous solution using UV/ZnO nano-photocatalysis and adsorption, *Journal of Molecular Liquids*, **2016**, 213, 374-380.

62- A. N. Amro, M. K. Abhary, M. M. Shaikh, S. Ali, Removal of Lead and Cadmium Ions from Aqueous Solution by Adsorption on a Low-Cost Phragmites Biomass, *Processes*, **2019**, 7, 406-417.

63- H. K. Hami, R. F. Abbas, A. A. Waheb, M. A. Abed, A. A. Maryoosh, Isotherm and pH Effect Studies of Tetracycline Drug Removal from Aqueous Solution Using Cobalt Oxide Surface, *Al-Nahrain Journal of Science*, **2019**, 22, 12-18.

64- F. F. Al-Qaim, Adsorption of Malachite Green (MG) on low cost–adsorbent from aqueous solution, *Journal of Babylon University for Pure Applied Sciences*, **2011**, 1, 48-56.

65- S. K. Ghati, Removal of Chlorpyrifos (Dursban) Pesticide from Aqueous Solutions using Barley Husks, *Ibn al-Haitham Journal for Pure and Applied Science*, **2017**, 29, 54-68.

66- E. A. Assirey, S. M. Sirry, H. A. Burkani, M. Ibrahim, Biosorption of Zinc (II) and Cadmium (II) Using Ziziphus Spina Stones, *Journal of Computational Theoretical Nanoscience*, **2018**, 15, 3102-3108.

67- S. Afroze, T. K. Sen, H. M. Ang, Adsorption removal of zinc (II) from aqueous phase by raw and base modified Eucalyptus sheathiana bark: Kinetics, mechanism and equilibrium study, *Process Safety and Environmental Protection*, **2016**, 102, 336-352.

68- Y.-S. Ho and G. McKay, Pseudo-second order model for sorption processes, *Process biochemistry*, **1999**, 34, 451-465.

69- A. Taha, E. Da'na, H. A. Hassanin, Modified activated carbon loaded with bio-synthesized Ag/ZnO nanocomposite and its application for the removal of Cr (VI) ions from aqueous solution, *Surfaces and Interfaces*, **2021**, 23, 100928.

70- O. Aworanti, S. Agarry, Kinetics, isothermal and thermodynamic modelling studies of hexavalent chromium ions adsorption from simulated wastewater onto Parkia biglobosa-Sawdust derived acid-steam activated carbon, *Methods*, **2017**, 10, 11.

71- H. E. I. Ismi, A. Ouass, L. Chafki, H. Essebaai, H. Bousfiha, A. Lebkiri, E. H. Rifi, Kinetic Analysis and Isotherm Modeling for the Adsorption of Silver Ion from Aqueous Solution on a Superabsorbent Polymer, *J. Mater. Environ. Sci.*, **2017**, 8, 4705-4715.

72- S. Agarry, O. Ogunleye, O. Ajani, Biosorptive removal of cadmium (II) ions from aqueous solution by chemically modified onion skin: batch equilibrium, kinetic and thermodynamic studies, *Chemical Engineering Communications*, **2015**, 202, 655-673.

73- C. Veloso, L. Filippov, I. Filippova, S. Ouvrard, A. Araujo, Technology, Adsorption of polymers onto iron oxides: Equilibrium isotherms, *Journal of Materials Research*, **2020**, 9, 779-788.

74- M. Uzqueda, A. Zornoza, J. R. Isasi, C. Martín, M. Sánchez, I. Vélaz, Interactions of terbinafine with β-cyclodextrin polymers: sorption and release studies, *Journal of Inclusion Phenomena and Macrocyclic Chemistry*, **2011**, 69, 469-474.